JOURNAL OF VIROLOGY, May 2007, p. 4928–4940 Vol. 81, No. 10
0022-538X/07/$08.00+0 doi:10.1128/JVI.02632-06

The CD8$^+$ T-Cell Response to Lymphocytic Choriomeningitis Virus Involves the L Antigen: Uncovering New Tricks for an Old Virus$^{\nabla}$†

Maya F. Kotturi,[1] Bjoern Peters,[1] Fernando Buendia-Laysa, Jr.,[1] John Sidney,[1] Carla Oseroff,[1] Jason Botten,[2] Howard Grey,[1] Michael J. Buchmeier,[2] and Alessandro Sette[1]*

Division of Vaccine Discovery, La Jolla Institute for Allergy and Immunology, 9420 Athena Circle, La Jolla, California 92037,[1] and Molecular and Integrative Neurosciences Department, The Scripps Research Institute, 10550 North Torrey Pines Road, La Jolla, California 92037[2]

Received 28 November 2006/Accepted 14 February 2007

CD8$^+$ T-cell responses control lymphocytic choriomeningitis virus (LCMV) infection in H-2^b mice. Although antigen-specific responses against LCMV infection are well studied, we found that a significant fraction of the CD8$^+$ CD44^{hi} T-cell response to LCMV in H-2^b mice was not accounted for by known epitopes. We screened peptides predicted to bind major histocompatibility complex class I and overlapping 15-mer peptides spanning the complete LCMV proteome for gamma interferon (IFN-γ) induction from CD8$^+$ T cells derived from LCMV-infected H-2^b mice. We identified 19 novel epitopes. Together with the 9 previously known, these epitopes account for the total CD8$^+$ CD44^{hi} response. Thus, bystander T-cell activation does not contribute appreciably to the CD8$^+$ CD44^{hi} pool. Strikingly, 15 of the 19 new epitopes were derived from the viral L polymerase, which, until now, was not recognized as a target of the cellular response induced by LCMV infection. The L epitopes induced significant levels of in vivo cytotoxicity and conferred protection against LCMV challenge. Interestingly, protection from viral challenge was best correlated with the cytolytic potential of CD8$^+$ T cells, whereas IFN-γ production and peptide avidity appear to play a lesser role. Taken together, these findings illustrate that the LCMV-specific CD8$^+$ T-cell response is more complex than previously appreciated.

A central feature of CD8$^+$ T-cell responses is immunodominance, a phenomenon by which only a subset of the potentially immunogenic peptides in an antigen are in fact recognized following natural infection or deliberate immunization (33). Experimental infection of laboratory mice with lymphocytic choriomeningitis virus (LCMV) is a widely utilized system for studying the mechanisms of immunodominance in viral infection (3, 24, 29, 31). Viral clearance in the course of acute LCMV infection in the mouse is critically dependent upon the CD8$^+$ cytotoxic T lymphocyte (CTL) response. Following acute infection of C57BL/6J (H-2^b) mice with the Armstrong strain of LCMV, a large proportion of the viral CD8$^+$ T-cell response is directed against two epitopes derived from the glycoprotein (GP) (amino acids 33 to 41) and the nucleoprotein (NP) (amino acids 396 to 404), as well as several other epitopes, including GP34-41, GP276-286, GP118-125, GP92-101, and NP205-212 (7, 31). Recent data demonstrate that, following acute LCMV infection, 85 to 95% of CD8$^+$ T cells are CD44^{hi} and that the known LCMV epitopes plus the newly defined GP70-77, NP166-175, and NP235-243 account for only about 80% of this CD8$^+$ CD44^{hi} T-cell pool (17). Thus, based on these studies (which were restricted to the NP and GP gene products), some questions remain on the possible contribution of non-LCMV-specific T cells recruited by bystander activation to the CD8$^+$ CD44^{hi} T-cell pool.

The products of the L-RNA segment, L (RNA polymerase) and Z (Zinc binding protein), have been discounted as a potential source of CTL epitopes because of the reported low expression of L (10, 12) and the small size of Z. Indeed, previous studies searching for novel CD8$^+$ T-cell responses to LCMV infection in H-2^b mice have found a narrow response because they concentrated on identifying epitopes derived from the viral GP and NP. To the best of our knowledge, a systematic study has not been undertaken, and the immunogenicity of the L and Z proteins for CD8$^+$ T-cell responses has not been fully characterized.

Recent data from our laboratory (19, 22) and others (1, 9) have shown that the overall breadth of CD8$^+$ T-cell responses to diverse viral pathogens might be more complex than previously appreciated. Analysis of the anti-vaccinia virus (VACV) CD8$^+$ T-cell response in HLA-transgenic mice infected with VACV and humans vaccinated against smallpox has revealed that CD8$^+$ T cells recognize a large repertoire of antigenic determinants distributed among multiple vaccinia proteins (19, 21, 22). Similar approaches to identify potential CD8$^+$ T-cell epitopes of human cytomegalovirus (CMV) have also demonstrated that a sizeable number of human CMV proteins encode numerous T-cell determinants; computer-based algorithms and enzyme-linked immunospot (ELISPOT) analyses identified epitopes in 14 distinct human CMV proteins (9, 27). Humans infected with other complex pathogens, such as *Plasmodium falciparum*, influenza A, and human immunodeficiency virus type 1 also develop multiepitope-specific CD8$^+$ T-cell responses to these infections (1, 8, 14). Thus, it appears that the responses to broad repertoires of epitopes shape both

* Corresponding author. Mailing address: La Jolla Institute for Allergy and Immunology, 9420 Athena Circle, La Jolla, CA 92037. Phone: (858) 752-6916. Fax: (858) 752-6985. E-mail: alex@liai.org.
† Kirin publication number 789.
$^{\nabla}$ Published ahead of print on 28 February 2007.

human and mouse $CD8^+$ T-cell immunodominance during infection.

Based on these data, we investigated whether the repertoire of responses to LCMV might be broader than previously appreciated. Initial data generated in our laboratory consistent with the recent report of Masopust et al. (17) indicated that a significant fraction of the $CD8^+$ $CD44^{hi}$ response in the H-2^b system could not be accounted for by known epitopes. Accordingly, we examined whether the LCMV-specific $CD8^+$ T-cell response in H-2^b mice is indeed focused on the relatively few previously described epitopes or whether the response encompasses a broader repertoire of yet unknown epitopes. Algorithms that predict peptides capable of binding to major histocompatibility complex (MHC) are routinely used to identify CTL epitopes derived from a diverse array of viral pathogens (4, 9, 21, 22, 25). We have applied this approach successfully to identify epitopes responsible for about 95% of the total $CD8^+$ T-cell response in the VACV system (19). To complement the predictive algorithm approach, we also used a set of overlapping 15-mer peptides spanning the entire LCMV proteome. This allowed us to expand our search to epitopes of noncanonical size or motif and to directly compare the two most widely used epitope identification methods.

We used different epitope identification methods in combination with functional assays for enumerating $CD8^+$ T cells (gamma interferon [IFN-γ] ELISPOT and intracellular staining for IFN-γ) and screened more than 1,000 peptides. As a result, we describe here the identification of 19 novel LCMV-specific epitopes. Of these epitopes, most are derived from the L protein. The new epitopes account for a large fraction of the total LCMV-specific response. The sum of the previously known epitopes and the 19 newly identified epitopes seem to account for the total $CD8^+$ $CD44^{hi}$ response obtained in LCMV-infected H-2^b mice.

MATERIALS AND METHODS

Peptide synthesis. Peptides were synthesized as crude material by Pepscan Systems (Lelystad, The Netherlands) as described previously (26). A total of 400 K^b and D^b algorithm-selected peptides, along with a set of 664 15-mer peptides, overlapping by 10 amino acids, spanning the entire LCMV proteome, were synthesized. The set of 664 15-mers were separated into 83 pools containing 8 peptides per pool. Candidate epitopes were identified in pool deconvolution studies. For mapping the minimal epitope within each positive 15-mer peptide, an additional set of 550 peptides of 8, 9, 10, and 11 amino acids in length were synthesized. Optimal LCMV-specific epitopes were resynthesized by A and A Labs and purified to 95% or greater homogeneity by reverse-phase high-performance liquid chromatography.

MHC peptide-binding assay. Quantitative assays to measure the binding affinity of peptides to purified K^b and D^b molecules are based on the inhibition of binding of a radiolabeled standard peptide and were performed essentially as described elsewhere (26, 32). After a 2-day incubation, binding of the radiolabeled peptide to the corresponding MHC class I molecule was determined by capturing MHC-peptide complexes on Greiner Lumitrac 600 microplates (Greiner Bio-One, Monroe, NC) coated with either Y-3 antibody (Ab) (K^b) or 28-14-8S Ab (D^b) and measuring bound cpm using the Topcount microscintillation counter (Packard Instruments).

Bioinformatic analyses. Experimental data of peptides binding to H-2^b molecules previously generated in our laboratory were used to develop binding predictions. This data set comprised 521 8-mer and 230 9-mer peptides binding to K^b and 319 9-mer peptides and 149 10-mer peptides binding to D^b. In addition, combinatorial peptide libraries described in reference 30 were available for peptides of 8 and 9 amino acids in length binding to K^b and 9 amino acids in length binding to D^b. These two sources of data were combined to calculate scoring matrices that quantify the contribution of each residue in a fixed-length peptide to binding to an MHC molecule, as described in detail in reference 23. The entire proteome of LCMV Armstrong (clone 53b) was then scanned for peptides of 8, 9, and 10 amino acids in length. The MHC binding affinity of these peptides was predicted using the scoring matrices described above, and peptides with affinities in the top 3% were synthesized as potential epitope candidates.

Mice. C57BL/6J and B6.SJL/J female mice (The Jackson Laboratory, Bar Harbor, ME) were housed in the animal facilities at the La Jolla Institute for Allergy and Immunology (San Diego, CA) and were used between 6 to 12 weeks of age. All mouse studies followed guidelines set out by the National Institutes of Health and Institutional Animal Care and Use Committee-approved animal protocols.

Virus. The Armstrong clone 53b strain of LCMV was obtained from Matthias G. von Herrath (La Jolla Institute for Allergy and Immunology). The LCMV stock was prepared in BHK-21 cells, and viral titer was determined through plaque assays on Vero cells in three independent experiments.

Infection and immunization. B6 mice were infected intraperitoneally (i.p.) with 1×10^4 to 1×10^5 PFU of LCMV in phosphate-buffered saline (PBS). At 8 days postinfection, mice were sacrificed, and purified splenic $CD8^+$ T cells or splenocytes were used for ex vivo mouse IFN-γ ELISPOT or for IFN-γ intracellular cytokine staining (ICCS) assays, respectively. For peptide immunization, mice were immunized subcutaneously with a mixture of peptide (50 μg/mouse) and the helper IA^b-restricted epitope, hepatitis B virus (HBV) core 128 to 140 (140 μg/mouse) (18) in PBS–9.5% dimethyl sulfoxide (DMSO) emulsified in incomplete Freund's adjuvant. After 12 days, mice were challenged with 1×10^5 PFU LCMV i.p. On day 4 postchallenge, titers were determined from the spleen by plaque assays on Vero cells. Virus titers were calculated per gram of spleen.

Ex vivo IFN-γ ELISPOT assay. The mouse IFN-γ ELISPOT assay was performed as previously described (28). Each assay was performed in triplicate wells, and the experimental values were expressed as the mean net spots/10^6 $CD8^+$ T cells ± standard error of the mean for each peptide tested. Responses against DMSO alone were measured to establish background values that were subtracted from experimental values. Statistical significance was determined by a Student's t test. For all tests, a P value of ≤ 0.05 using the mean of triplicate values of the response against the relevant peptide versus the response against DMSO alone was considered to indicate statistical significance. The net number of spots/10^6 effector cells was calculated as follows: [(number of spots against relevant peptide) − (number of spots against DMSO control)] × [(1×10^6)/(number of effector cells/well)]. The stimulation index (SI) was calculated as follows: (number of spots against relevant peptide)/(number of spots against DMSO control).

Intracellular IFN-γ staining. Splenocytes from day 8 LCMV-infected B6 mice were cultured in the presence of 10 pg/ml to 1 μg/ml of MHC class I peptide, 10 μg/ml brefeldin A (BFA; Sigma-Aldrich), and 50 U/ml recombinant human interleukin-2 (rhIL-2; Roche, Palo Alto, CA) in complete medium. After 5 h, cells were harvested and stained with allophycocyanin-conjugated anti-mouse CD8α monoclonal Ab (MAb, clone 53-6.7; BD Biosciences, San Jose, CA). In some experiments, cells were also stained with fluorescein isothiocyanate-conjugated anti-mouse CD44 MAb (clone IM7; BD Biosciences). Cells were fixed and permeabilized and then stained for intracellular IFN-γ and tumor necrosis factor alpha (TNF-α) with a phycoerythrin-conjugated anti-mouse IFN-γ MAb (clone XMG1.2; BD Biosciences) and fluorescein isothiocyanate-conjugated anti-mouse TNF-α MAb (clone MP6-XT22; BD Biosciences), respectively. After washing, samples were resuspended in 1% paraformaldehyde–PBS and acquired on a FACSCalibur flow cytometer (BD Biosciences). The frequency of $CD8^+$ T cells responding to each MHC class I peptide was quantified by determining the percent total of gated $CD8^+$ and IFN-γ^+ or TNF-α^+ cells using CellQuest software (Becton Dickinson, San Jose, CA). The peptide-specific responses were calculated by subtracting the percentage of cells that scored positive for IFN-γ or TNF-α^+ production in the absence of peptide (no peptide control).

In vivo cytotoxicity assay. Splenocytes from naive B6.SJL/J mice were treated with red blood cell lysing buffer, washed, and divided into two equal cell populations at 10×10^6 cells/ml. One group of cells was incubated with the relevant CTL peptide at 0.5 μg/ml (targets) and the other group with DMSO (marker population) for 90 min at 37°C. Cells were washed and resuspended at 10×10^6 cells/ml with PBS–0.1% bovine serum albumin. Target and marker cell populations were incubated with 1.0 μM and 100 nM CFSE (Invitrogen Molecular Probes, Carlsbad, CA), respectively, for 10 min at 37°C. Excess CFSE was removed by washing, the two cell populations were combined in 1:1 ratio, and 10×10^6 total cells were adoptively transferred intravenously into day 8 LCMV-infected recipient B6 mice. After 5 h, spleens were harvested from recipient mice. Splenocytes were stained with biotin-conjugated mouse anti-CD45.1 MAb (clone A20; BD Biosciences), followed by streptavidin-allophycocyanin conjugate to further differentiate donor cells from recipient. The ratio of target

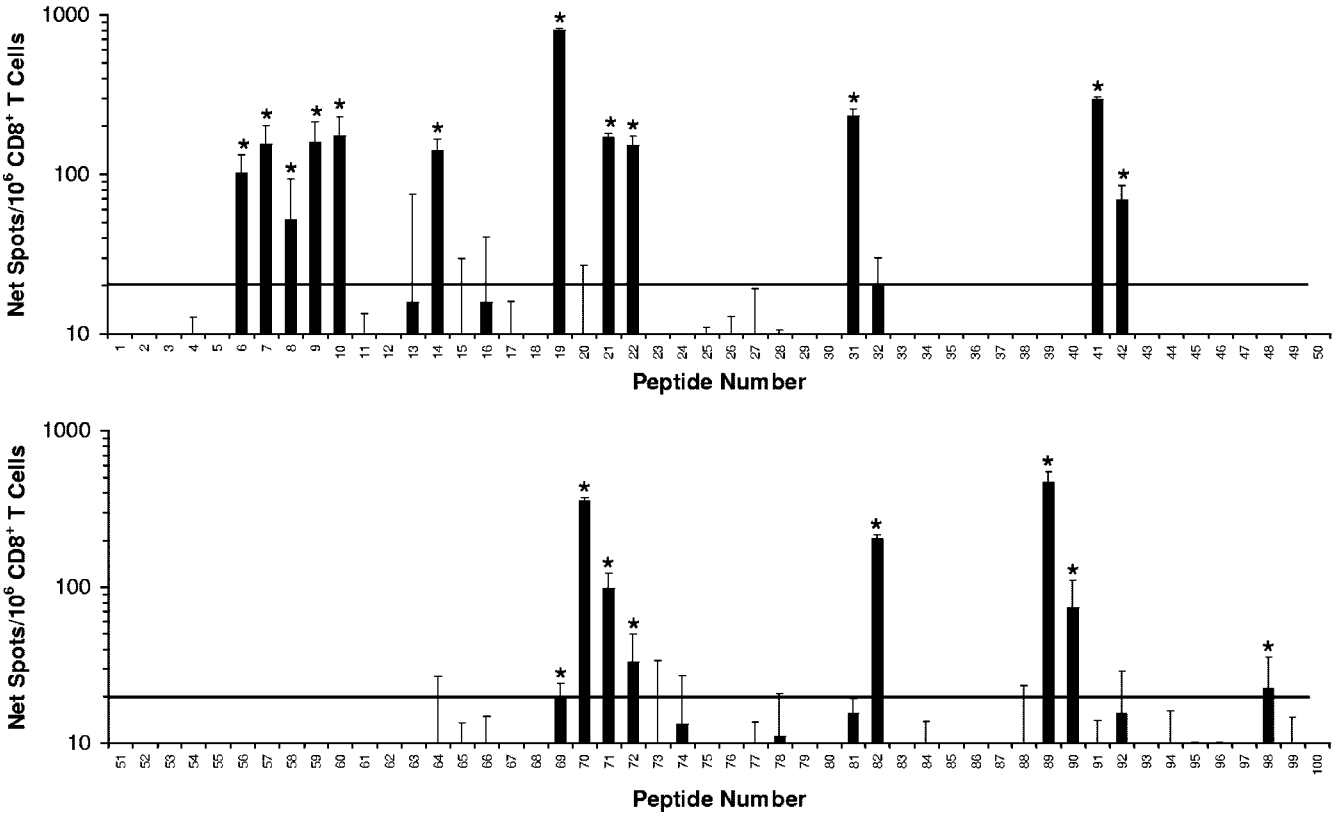

FIG. 1. Representative screen of individual K^b 9-mer peptides derived from the LCMV Armstrong proteome. The criteria for positivity were an SI of ≥2.0 and net SFCs/10^6 cells of ≥20 in duplicate assays. The line at 20 net SFCs/10^6 cells indicates the threshold used to define positivity. An asterisk indicates positive peptides. In total, 20 of 100 K^b 9-mer peptides were positive in the IFN-γ ELISPOT assay. The number of positive K^b 9-mer peptides was reduced to 18 after removing nested peptides containing the same core sequence but producing a lower response in the assay.

($CFSE^{high}$) to marker ($CFSE^{low}$) donor cells was assessed by flow cytometry on a FACSCalibur. Specific killing was calculated as follows: 100 − [(target-to-marker ratio in LCMV-infected mice × 100)/(target-to-marker ratio in naive mice)].

RESULTS

$CD8^+$ $CD44^{hi}$ T-cell response in LCMV-infected H-2^b mice. In preliminary experiments, a total of 91% of $CD8^+$ $CD44^{hi}$ T cells were detected in splenocytes from day 8 LCMV-infected H-2^b mice. In contrast, we observed repeatedly that a maximum of 45% of $CD8^+$ T cells could produce IFN-γ in response to all of the previously characterized epitopes (GP33-41, GP34-41, GP276-286, GP118-125, GP92-101, NP205-212, NP166-175, and NP235-243), except GP70-77, which did not evoke a significant IFN-γ response over background.

This discrepancy might be due to the presence of unaccounted antigen-specific $CD8^+$ T cells or cytokine-mediated bystander activation. Experiments using LCMV-infected MHC class I-matched cells as stimulators to enumerate antigen-specific $CD8^+$ $CD44^{hi}$ T cells yielded highly variable results (data not shown). Therefore, we chose to search for the additional antigen-specific $CD8^+$ T cells by screening the antigenicity of LCMV-derived peptides predicted to bind to either K^b or D^b molecules.

Identification of LCMV-derived potential $CD8^+$ epitopes using predicted peptides. A total of 400 predicted determinants were synthesized, comprising the top 100 each of K^b 8-mers and 9-mers and D^b 9-mers and 10-mers. The antigenicity of these predicted peptides was assessed at the peak of the primary T-cell response by using purified splenic $CD8^+$ T cells from B6 mice 8 days after i.p. infection with LCMV. Antigenicity was evaluated by measuring IFN-γ spot formation in at least two independent ELISPOT assays utilizing 0.5 and 10 μg/ml of each peptide. Representative data from the screen of the 100 K^b 9-mer peptides tested at 0.5 μg/ml is shown in Fig. 1. Peptides with an average of ≥20 spot-forming cells (SFCs)/10^6 $CD8^+$ T cells and an average SI of ≥2.0 in replicate assays were considered positive. Using this approach, we identified 18 K^b 8-mer, 14 K^b 9-mer, 11 D^b 9-mer, and 5 D^b 10-mer potential epitopes. Of these, two corresponded to the well-characterized NP epitopes, NP396-404 and NP205-212, and five were previously characterized GP epitopes (GP33-41, GP34-41, GP118-125, GP92-101, and GP70-77) (data not shown).

Identification of LCMV-derived $CD8^+$ epitopes using overlapping 15-mer peptides. Previous work has established that $CD8^+$ T-cell epitopes can be identified by using overlapping peptides spanning complete viral proteomes (1, 27). Herein, we measured the antigenicity of a library of 15-mer peptides,

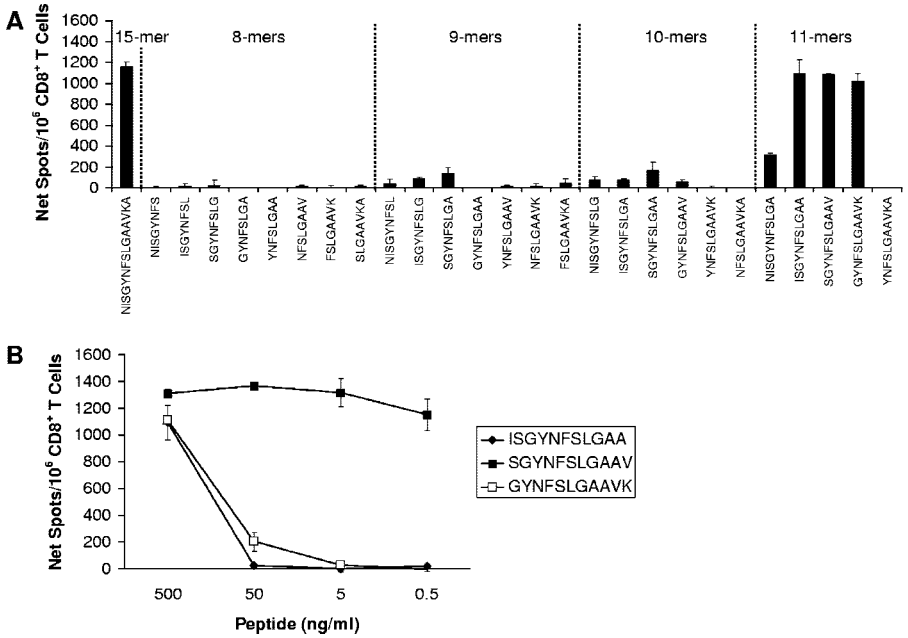

FIG. 2. Representative screen of optimal determinants within an antigenic 15-mer peptide. (A) The optimal epitope was mapped within a 15-mer peptide, NP236-250, by analyzing $CD8^+$ T-cell responses to a series of truncated peptides, including eight 8-mers, seven 9-mers, six 10-mers and five 11-mers (separated by dotted lines) in an IFN-γ ELISPOT assay using purified splenic $CD8^+$ T cells from LCMV-infected B6 mice 8 days postinfection. The amino acid sequence of each peptide is indicated. Three highly antigenic 11-mer peptides, NP237-247, NP238-248, and NP239-249, were detected. (B) Dose-dependent $CD8^+$ T-cell responses to the three antigenic 11-mer peptides were analyzed by IFN-γ ELISPOT assay to pinpoint the optimal 11-mer epitope. Only NP238-248 remained antigenic at low peptide doses and was therefore defined as the optimal epitope within the 15-mer peptide.

overlapping by 10 amino acids that spanned the entire LCMV Armstrong proteome. This method was utilized to confirm putative epitopes identified by the predictive approach and also to identify potentially novel epitopes overlooked by the predictive approach.

A set of 664 15-mer peptides was divided into 83 peptide pools with 8 peptides per pool. The antigenicity of these pools was evaluated in two independent IFN-γ ELISPOT assays using purified splenic $CD8^+$ T cells from day 8 LCMV-infected B6 mice. The two peptide pools spanning the Z protein were not positive in these assays. By contrast, 24 pools derived from the NP, GP, and L proteins generated positive responses following LCMV infection. A total of 42 15-mer peptides generated reproducible responses (data not shown). Each peptide pool contained one or more positive 15-mer peptide(s), except one pool, for which no definitive individual peptide stimulating a response could be identified.

Optimal epitopes map within antigenic 15-mer peptides. Of the 42 antigenic 15-mers, 25 were nested and produced a similar $CD8^+$ T-cell response to an already identified predicted minimal peptide (data not shown). In several cases, two overlapping 15-mer peptides matched a single predicted determinant, thus decreasing the number of candidates from 25 to 16. Furthermore, 17 antigenic 15-mers did not contain a predicted peptide. To identify the optimal candidate epitope within each of these "unmatched" 15-mer peptides, sets of 8-mers, 9-mers, 10-mers, and 11-mers were synthesized and tested in the IFN-γ ELISPOT assay using purified splenic $CD8^+$ T cells from day 8 LCMV-infected B6 mice as effectors.

Representative data for the truncated peptides derived from the NP236-250 15-mer are shown in Fig. 2A. At the 0.5-μg/ml dose, three peptides of 11 amino acids in length were able to activate $CD8^+$ T cells to a level similar to that of NP236-250, whereas the remaining peptides generated either weak or no responses. The optimal 11-mer peptide was mapped to NP238-248 by analyzing the dose-dependent $CD8^+$ T-cell response to these three 11-mer peptides (Fig. 2B). Of these 11-mers, NP238-248 was the only peptide capable of activating $CD8^+$ T cells at both 5 and 0.5 ng/ml.

Accordingly, we identified an additional seven optimal peptides (data not shown). No clear candidate epitope could be identified for 10 of the unmatched antigenic 15-mer peptides, because of weak and/or inconsistent results with the original 15-mer and/or truncated peptide sets. The well-characterized GP-specific D^b 11-mer epitope, GP276-286, was independently identified here. We also identified two NP-specific 11-mers, NP165-175 and NP238-248, that were similar to the previously known D^b 8-mer, NP166-173, and K^b 9-mer, NP235-243, respectively. In addition, we identified 4 novel L protein-derived determinants, including 2 K^b 8-mers, 1 K^b 11-mer, and 1 D^b 11-mer. These potential epitopes were missed by the predictive approach because they contained a noncanonical K^b motif (8-mers) or were of noncanonical size (11-mers).

Enumeration of antigen-specific $CD8^+$ T cells during LCMV infection. In summary, the prediction approach identified 48 candidate epitopes. The overlapping peptide approach identified a total of 23 potential epitopes. A combined total of 55 unique putative LCMV-specific determinants were detected by both epitope identification methods, the majority of which were newly identified and derived from the L protein (data not shown). To

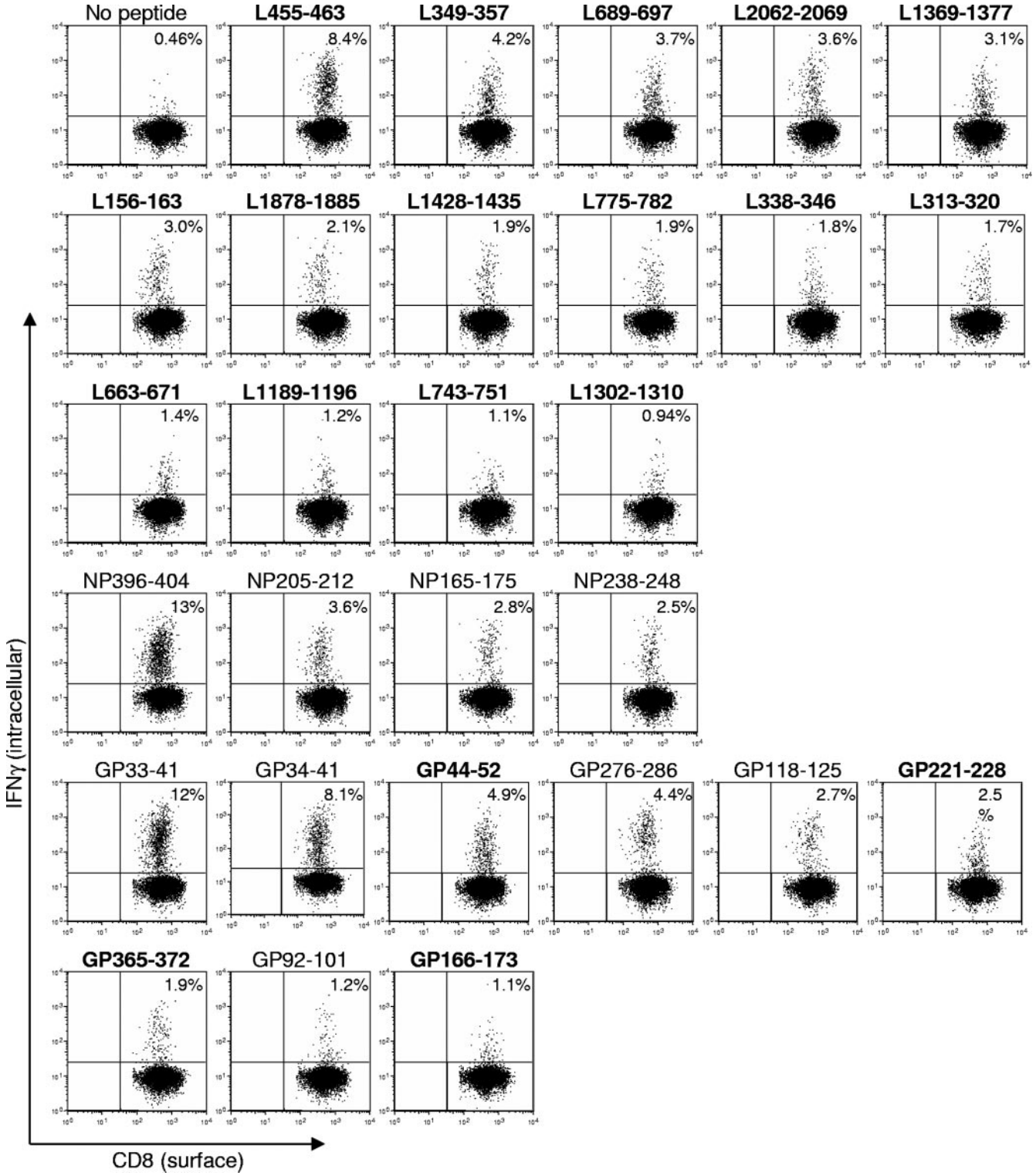

FIG. 3. Frequency of $CD8^+$ IFN-γ^+ T cells against newly identified and known epitopes during LCMV infection. B6 mice were infected i.p. with LCMV. Day 8 postinfection splenocytes were harvested and stimulated in vitro with or without the indicated peptides at 0.1 μg/ml (boldface type indicates novel epitopes) in the presence of BFA and rhIL-2. Intracellular IFN-γ staining was used to enumerate the number of antigen-specific $CD8^+$ T cells. A representative analysis for each epitope is shown, where the percentage of $CD8^+$ T cells that stain positive for IFN-γ is indicated in the upper right quadrant.

TABLE 1. Summary of characteristics of LCMV-derived epitopes

Antigen name[a] (peptide position)	Peptide sequence	Restriction size	ELISPOT assay (SFC/10^6 cells)	ICCS assay (% $CD8^+$ IFN-γ^+ cells)[b]	In vivo CTL assay (% specific killing)	Prediction ranking[d]	Binding affinity (IC_{50} nM)[e]	
							K^b	D^b
GP118-125	ISHNFCNL	Kb 8-mer	826	2.1	ND[c]	1	1.5	8,870
GP166-173	**ITIQYNLT**	**Kb 8-mer**	**191**	**0.59**	**ND**	**18**	**35.2**	**7,390**
GP221-228	**SQTSYQYL**	**Kb 8-mer**	**209**	**2.8**	**7.8**	**27**	**7.8**	**64,500**
GP34-41	AVYNFATC	Kb 8-mer	8,923	8.2	ND	28	1.2	1,320
GP365-372	**MGVPYCNY**	**Kb 8-mer**	**265**	**1.2**	**ND**	**38**	**5,740**	**88,000**
L156-163	**ANFKFRDL**	**Kb 8-mer**	**801**	**1.7**	**62**	**6**	**4.6**	**70,000**
L313-320	**TSTEYERL**	**Kb 8-mer**	**218**	**0.86**	**ND**	**7**	**34**	**80,100**
L775-782	**SSFNNGTL**	**Kb 8-mer**	**163**	**0.94**	**11**	**24**	**104**	**2,650**
L2062-2069	**RSIDFERV**	**Kb 8-mer**	**931**	**2.5**	**98**	**26**	**1.1**	**88,000**
L1189-1196	**MMCPFLFL**	**Kb 8-mer**	**85**	**0.56**	**ND**	**29**	**246**	**26,300**
L1428-1435	**NSIQRRTL**	**Kb 8-mer**	**60**	**1.2**	**4.3**	*****	**58,794**	**70,000**
L1878-1885	**GPFQSFVS**	**Kb 8-mer**	**815**	**1.3**	**59**	*****	**46**	**70,000**
NP205-212	YTVKYPNL	Kb 8-mer	885	2.8	ND	3	0.55	70,000
L1302-1310	**INYCIGVIF**	**Kb 9-mer**	**102**	**0.45**	**ND**	**6**	**86**	**30,600**
L743-751	**VFYEQMKRF**	**Kb 9-mer**	**155**	**0.64**	**ND**	**7**	**344**	**78,500**
L663-671	**VVYKLLRFL**	**Kb 9-mer**	**51**	**1.4**	**ND**	**8**	**43**	**3,460**
L1369-1377	**FAAEFKSRF**	**Kb 9-mer**	**171**	**2.5**	**ND**	**21**	**25**	**6,040**
L349-357	**SSLIKQSKF**	**Kb 9-mer**	**150**	**4.4**	**5.6**	**22**	**472**	**4,720**
GP44-52	**FALISFLLL**	**Db 9-mer**	**65**	**4.0**	**4.9**	**3**	**424**	**1.9**
GP33-41	KAVYNFATC	Db 9-mer	10,024	12.2	98	25	7,000	1,439
L338-346	**RQLLNLDVL**	**Db 9-mer**	**720**	**1.1**	**76**	**1**	**ND**	**0.15**
L455-463	**FMKIGAHPI**	**Db 9-mer**	**410**	**9.2**	**25**	**13**	**ND**	**188**
L689-697	**KFMLNVSYL**	**Db 9-mer**	**41**	**4.6**	**18**	**14**	**ND**	**11**
NP396-404	FQPQNGQFI	Db 9-mer	9,576	12.4	ND	2	4,240	0.23
GP92-101	CSANNSHHYI	Db 10-mer	537	0.42	ND	1	5,260	113
NP165-175	SSLLNNQFGTM	Db 11-mer	999	1.9	32	*	1,040	14,000
NP238-248	SGYNFSLGAAV	Kb 11-mer	1,313	1.8	91	*	0.38	172
GP276-286	SGVENPGGYCL	Db 11-mer	1,885	3.5	90	*	16,400	414

[a] Bold font highlights novel epitopes.
[b] Peptide tested at 0.1 μg/ml.
[c] ND, not determined.
[d] Asterisk indicates peptides identified only by 15-mer screening approach.
[e] Underlining indicates high- or intermediate-affinity binders ($IC_{50} < 500$ nM).

further examine the antigenicity of the 55 candidate epitopes defined in the ELISPOT assays, we tested them in an IFN-γ ICCS assay utilizing 0.1 μg/ml of peptide. Under these stringent conditions, a total of 28 different epitopes yielded positive results (at least >1.5 standard deviation above the average background). This threshold was based on the lowest standard deviation measured for the known epitopes. Nine of these were previously known (GP70-77 was negative), and 19 represent novel responses (representative data are shown in Fig. 3).

A total of 15 different L-specific novel epitopes were detected with responses in the 9.2 to 0.45% range (Table 1, background values are subtracted from the percentage of $CD8^+$ IFN-γ^+ cells averaged from two or more experiments). Of the four known NP epitopes identified, the overall strongest $CD8^+$ T-cell response was generated against the NP396-404 (12%) epitope and followed by NP205-213 (2.8%), NP165-175 (1.9%), and NP238-248 (1.8%). Within the seven GP-derived epitopes, five were previously known with responses in the 12 to 0.42% range and four (GP44-52, GP221-228, GP365-372, and GP166-173) with responses of 4.0%, 2.8%, 1.2%, and 0.59%, respectively, were novel.

Evaluation of relative efficacy and accuracy of different epitope identification methods. To assess the effectiveness of the predictive approach, the number of epitopes from Table 1 was plotted versus their rank for each H-2^b allele-size combination (Fig. 4). A strong correlation was observed between peptide antigenicity and prediction rank. In fact, each of the K^b 8-mer, D^b 9-mer, and D^b 10-mer with a prediction rank of one were antigenic, and all epitopes had a prediction rank of ≤38 (Table 1). Therefore, testing the top 1.2% (equivalent to 40) highest-ranking predicted epitopes (from each allele-size com-

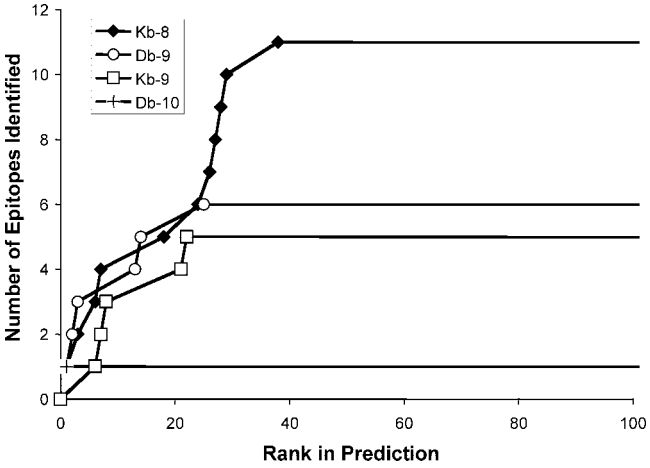

FIG. 4. Evaluation of bioinformatics prediction accuracy and sensitivity. Each line corresponds to the prediction for one H-2^b allele and peptide size. The *y* axis represents the number of epitopes that were identified as a function of the prediction rank of each epitope on the *x* axis. Epitope ranking is based on the predicted IC_{50}s for each epitope generated by the prediction algorithms.

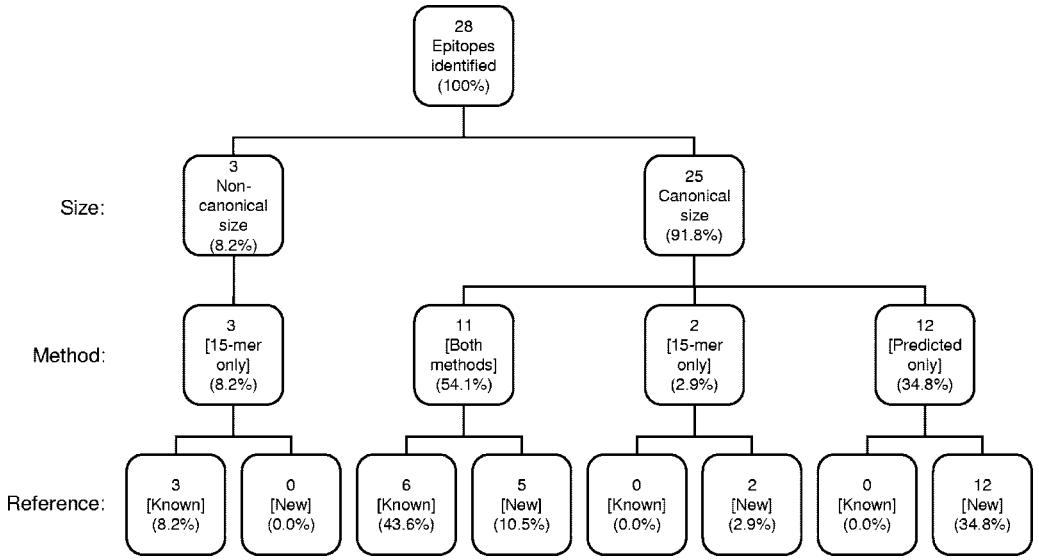

FIG. 5. Comparison of epitope identification methods. The 28 LCMV-specific epitopes are categorized by size (noncanonical versus canonical), method (predictive versus overlapping peptides), and reference (known versus new epitopes). The relative percentage of responding $CD8^+$ T cells to each group of epitopes is shown, where the additive percentage of $CD8^+$ T cells producing IFN-γ to each of the 28 individual epitopes is defined as 100% of the response.

bination) would have been sufficient to identify all 11 K^b 8-mers, 5 K^b 9-mer, 6 D^b 9-mers, and 1 D^b 10-mer epitopes. We also measured the binding capacity of the LCMV-specific epitopes identified through the predictive approach to their predicted H-2^b molecule (Table 1). Of these epitopes, 13 bound with high affinity (50% inhibitory concentration [IC_{50}] < 50 nM), 8 with intermediate affinity (IC_{50} < 500 nM), and 2 with low affinity (IC_{50} < 6,000 nM).

We then compared the effectiveness of the predictive approach to the overlapping peptide approach. A total of 28 unique epitopes were identified by predictive and overlapping peptide methods, which included 9 of the previously reported epitopes. The cumulative $CD8^+$ T-cell responses generated by individual peptide stimulation in the IFN-γ ICCS assays were defined as 100% of the response. Of the 28 epitopes identified by our analyses, the 3 noncanonical 11-mers made up 8.2% of the response (Fig. 5). The remaining 91.8% of the response was composed of 25 epitopes of canonical size. Of the canonical epitopes, 11 were identified by both methods (54.1%), 2 by 15-mer peptides only (2.9%), and the other 12 by predicted peptides only (34.8%).

In total, 54.1% of the anti-LCMV response is composed of epitopes that were identified by both methods. The 15-mer approach including truncated peptide sets required synthesis and testing of 1,214 peptides and identified approximately 65.2% of the overall response. By contrast, the predictive approach required synthesis and testing of 400 peptides (or 160 if only the top 1.2% from each allele would have been synthesized) and identified approximately 88.9% of the total response.

Further characterization of the new LCMV-specific epitopes. In the next series of experiments, the newly identified epitopes were further characterized in comparison to the previously known epitopes. First, we measured the frequency of TNF-α-producing cells. In agreement with a previous study, the percentage of TNF-α-producing $CD8^+$ T cells was consistently lower than that of IFN-γ (2); however, all 28 LCMV peptides generated a reproducible TNF-α response at 0.1 μg/ml (data not shown). Subsequently, we extended the IFN-γ ICCS dose-response studies to determine 50% effective concentrations (EC_{50}s, defined as the peptide concentration inducing 50% of the maximal $CD8^+$ T-cell response) for candidate known and new epitopes.

The $CD8^+$ T-cell responses directed against the NP-specific 11-mer epitopes, NP165-175 and NP238-248, and the well-characterized NP396-404 and NP205-212 were in a similar EC_{50} range (10 to 100 pg/ml) (Fig. 6A). The EC_{50}s for the newly identified GP221-228 and GP44-52 epitopes (100 ng/ml) were within the higher range of the 5 known GP-specific epitopes (50 pg/ml to 100 ng/ml) (Fig. 6B). The epitopes derived from the L protein had EC_{50}s (50 pg/ml to 100 ng/ml) (Fig. 6C) similar to the known GP- and NP-derived epitopes. Overall, these titration experiments demonstrated that peptide avidities of the newly identified LCMV-specific epitopes are within the same range as those of the known epitopes.

We also compared the frequency of memory $CD8^+$ T cells against the known and newly identified epitopes at 28, 115, and 239 days after LCMV infection. In general, long-term memory $CD8^+$ T-cell frequencies remained at approximately 20 to 40% of the day 8 response for all epitopes (data not shown). Taken together, these experiments show that the novel epitopes identified herein induce significant primary and memory $CD8^+$ T-cell responses as well as possessing similar peptide avidities to the previously characterized LCMV-derived epitopes.

Total size of antigen-specific $CD8^+$ T-cell response during LCMV infection. Intracellular IFN-γ staining was used to assess the percentage of LCMV-specific $CD8^+$ T cells responding to the known and new epitopes. Splenocytes from B6 mice 8 days after LCMV infection were cultured in vitro either without or with peptides at 0.1 μg/ml each for 5 h in the presence of BFA and

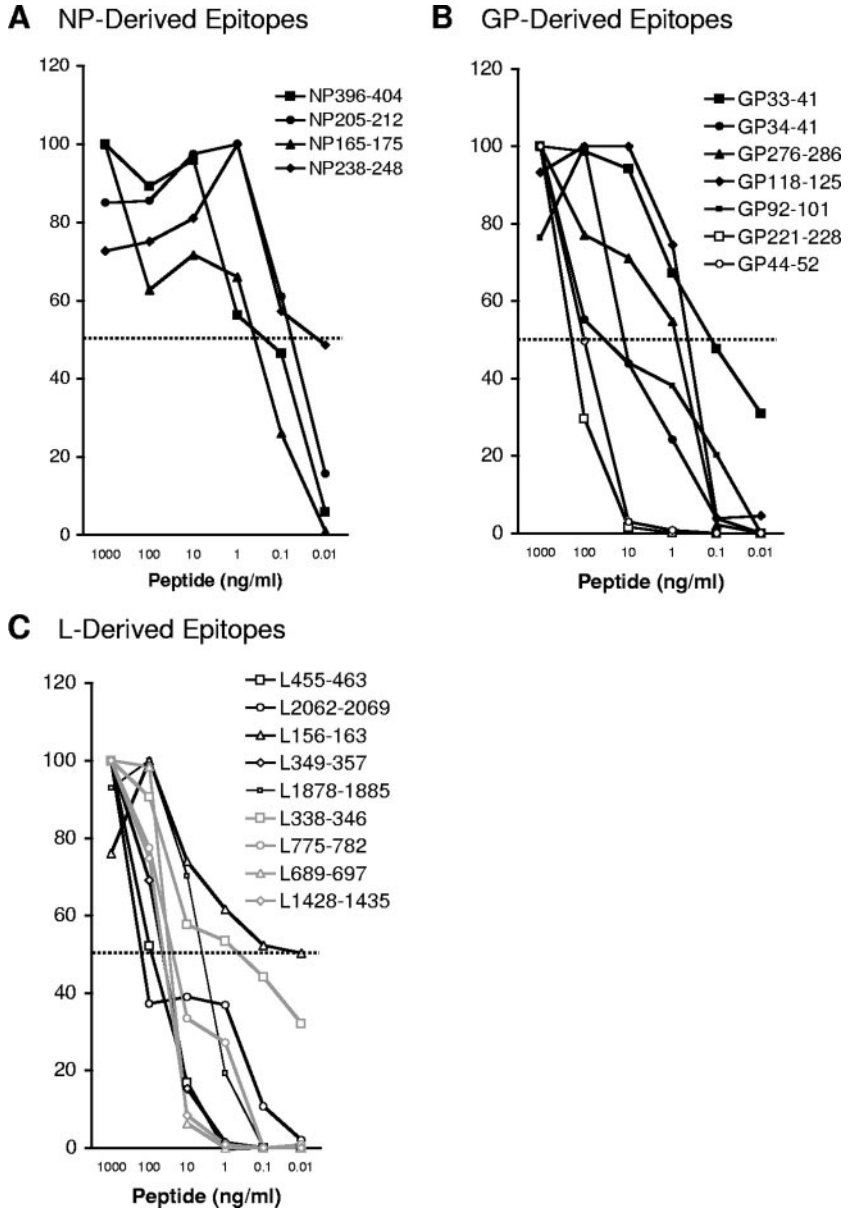

FIG. 6. $CD8^+$ T-cell dose-dependent response against known and newly identified LCMV-specific epitopes. Splenocytes from day 8 LCMV-infected mice were stimulated with candidate NP-specific peptides (A), GP-specific peptides (B), and L-specific peptides (C) from 10 pg/ml to 1 μg/ml. Intracellular IFN-γ staining was used to enumerate the number of antigen-specific $CD8^+$ T cells. Data are presented as relative percentages of $CD8^+$ T cells that produce IFN-γ following peptide stimulation, where 100% is defined as the maximal response regardless of the peptide dose tested. Closed markers indicate known epitopes, whereas open markers indicate newly identified epitopes. The dotted line indicates half of the maximal $CD8^+$ T-cell response, which was used to define the EC_{50} of each peptide. Data represent results from one of two or more independent experiments.

rhIL-2. A peptide dose of 0.1 μg/ml was utilized, since all of the known epitopes retained their activity at this concentration (Fig. 6). By adding $CD8^+$ T-cell responses generated by stimulation with individual peptides, we found that the 9 previously characterized epitopes (9 known) stimulated 45% of $CD8^+$ T cells, whereas the 19 newly identified epitopes (19 new) stimulated 42% of $CD8^+$ T cells (Fig. 7A). Notably, when responses to all 28 peptides were added together (9 known plus 19 new), 87% of $CD8^+$ T cells were stimulated. The data demonstrates that the T cells recognizing the new epitopes make up a significant portion (about one half) of the LCMV-specific response.

Next, we examined the sum total of $CD8^+$ T-cell responses directed against the 28 LCMV-specific epitopes, categorized by the viral antigen from which they were derived. Using peptides at 0.1 μg/ml, we found that NP epitopes stimulated 18% of $CD8^+$ T cells, whereas GP epitopes stimulated 35% of $CD8^+$ T cells (Fig. 7B). The L epitopes contributed to 34% of the $CD8^+$ T-cell response, again emphasizing that epitopes

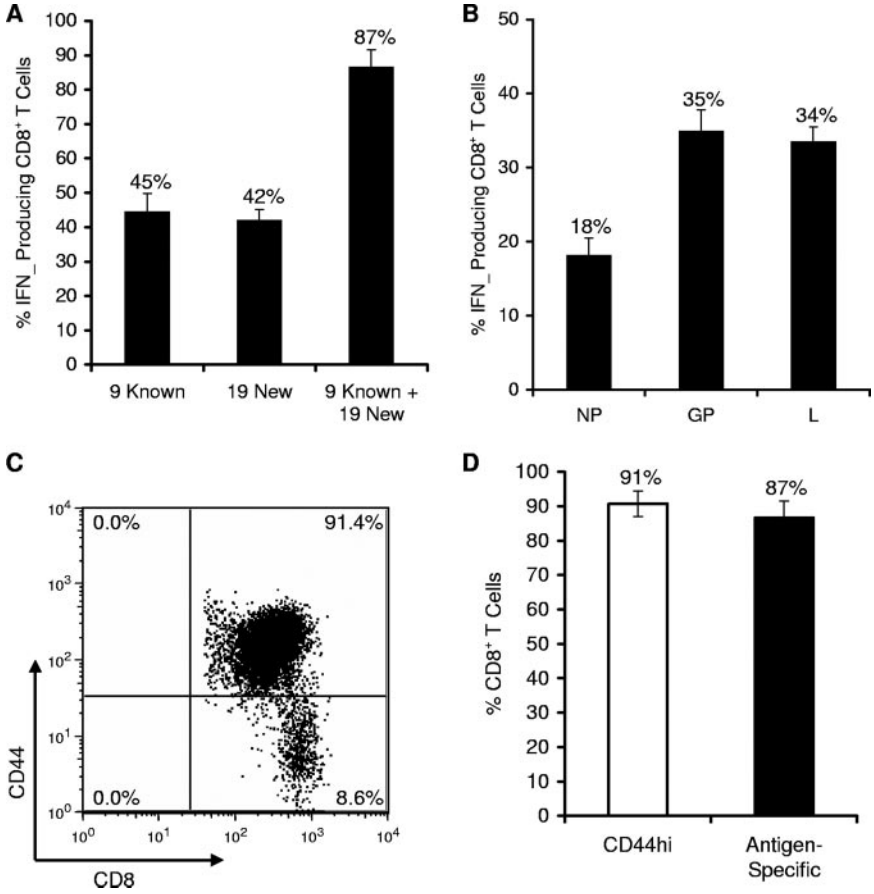

FIG. 7. Newly identified epitopes significantly contribute to overall magnitude of $CD8^+$ T cell response against LCMV. (A) Splenocytes from day 8 LCMV-infected mice were stimulated with individual peptides at 0.1 μg/ml. The percentage of $CD8^+$ T cells specific to either known or new epitopes was measured by intracellular staining for IFN-γ. The 9 previously characterized epitopes (9 known) consisted of the sum of responses against NP396-404, NP205-213, NP165-175, NP238-248, GP33-41, GP34-41, GP276-286, GP118-125, and GP92-101. The sum total response against the 19 new peptides was composed of GP44-52, GP221-228, GP365-372, GP166-173, L455-463, L349-357, L689-697, L2062-2069, L1369-1377, L156-163, L1878-1885, L1428-1435, L775-782, L338-346, L313-320, L663-671, L1189-1196, L743-751, and L1302-1310. (B) $CD8^+$ T-cell responses were categorized by viral antigen. The NP response is against 4 NP epitopes, GP response against 9 GP epitopes, and L response against 15 L epitopes. (C) Total percentage of $CD8^+$ $CD44^{hi}$ T cells from day 8 LCMV-infected mice. Splenocytes were stained for CD8 and CD44, and the percentage of double-positive cells is indicated in the upper right quadrant. Results are representative of six independent experiments. (D) Comparison of the percentage of $CD8^+$ $CD44^{hi}$ T cells to the percentage of epitope-specific $CD8^+$ IFN-γ^+ T cells from LCMV-infected B6 mice on day 8 postinfection.

derived from the L protein make up a significant portion of the overall $CD8^+$ T-cell response to LCMV.

Finally, we compared the percentage of antigen-specific $CD8^+$ T cells to the population of activated $CD8^+$ $CD44^{hi}$ T cells in the spleen. We found that approximately 91% ± 3.7% of $CD8^+$ T cells stain for CD44, which closely correlates with the frequency of $CD8^+$ T cells responding to the 28 epitopes identified in this study (Fig. 7C and D).

In vivo cytotoxic killing of L peptide-pulsed target cells during LCMV infection. After establishing that L-specific peptides are recognized by a significant fraction of $CD8^+$ T cells during LCMV infection of B6 mice, we examined the specific killing of L peptide-coated targets in vivo to further characterize the primary antiviral response against the L protein. Cytotoxicity was assessed by transferring peptide-labeled B6.SJL/J splenocytes into day 8 LCMV-infected B6 recipient mice.

After 5 h in vivo, we observed a 98% ± 2.2% and 90% ± 3.5% reduction in targets coated with the control GP33-41 and GP276-286 peptides, respectively, compared to the unlabeled marker population (representative data are shown in Fig. 8A). As expected, peptide-coated targets transferred into naive B6 mice were not killed. The specific killing induced by L455-463, L2062-2069, and L156-163 epitopes, which stimulated a high, medium, and low percentage of $CD8^+$ T cells compared to the known epitopes, respectively, was measured next. A high level of cytotoxicity (98% ± 0.80%) was observed against targets labeled with L2062-2069 (Fig. 8A), similar to the degree of cytotoxicity observed for GP33-41- and GP276-286-coated targets. A lower level of cytotoxicity was seen for L156-163 (62% ± 16%) and L455-463 (25% ± 14%) peptide-coated target cells.

We also observed that the level of killing did not correlate with the percentage of $CD8^+$ IFN-γ^+ T cells specific for the L455-463 epitope. To further investigate the relationship between cytolytic activity and IFN-γ production, the in vivo cytotoxic potential for 11 of the newly defined epitopes was

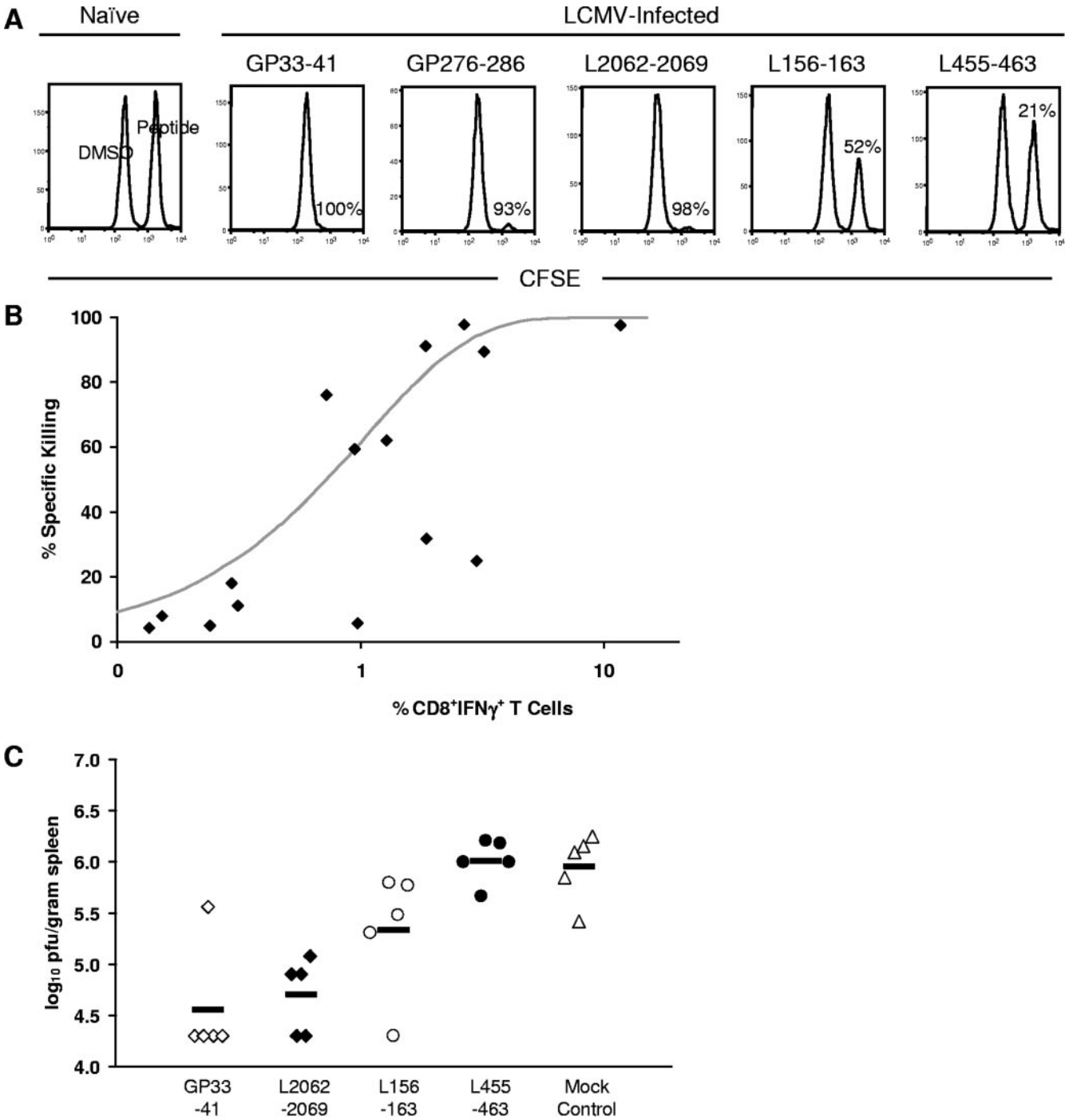

FIG. 8. Functional role of L epitopes in vivo during acute LCMV infection. (A) Specific in vivo cytotoxicity of L peptide-coated target cells. Day 8 LCMV-infected B6 mice were intravenously injected with CFSE-labeled target cells coated with GP33-41, GP276-286, L2062-2069, L455-463, or L156-163 peptide ($n = 3$). After 5 h, spleens were harvested and analyzed for specific killing of peptide-coated targets. Representative histograms for each peptide are gated on CD45.1$^+$ target cells in the spleen. Ratios of relevant peptide-coated (CFSE^{high}) and unlabeled marker (CFSE^{low}) donor cell populations were used to determine percentages of specific killing. Numbers correspond to the percentage of target cells killed. Data represent results from one of three independent experiments. (B) Comparison between cytotoxic activity and the percentage of antigen-specific CD8$^+$ T cells producing IFN-γ. Each square represents the percentage of specific killing and the percentage of CD8$^+$ IFN-γ$^+$ T cells for 11 of the newly defined LCMV epitopes, GP33-41, GP276-286, NP165-175, and NP238-248. (C) Impact of L peptide vaccination on virus titer. B6 mice were primed with GP33-41 (open squares), L2062-2069 (closed squares), L156-163 (open circles), L455-463 (closed circles), or mock control (open triangles) with DMSO emulsified in incomplete Freund's adjuvant ($n = 5$). Twelve days later, mice were challenged i.p. with 1×10^5 PFU LCMV. Virus titers were calculated per gram of spleen. When no plaque growth was detected, values were set at the threshold of detection ($\log_{10}$ PFU/gram spleen = 4.3). Horizontal lines indicate mean values. Results are representative of two independent experiments.

measured (the percentage of specific killing averaged from two experiments is shown in Table 1) and compared to GP33-41, GP276-286, NP165-175, and NP238-248. The averaged cytotoxicity values were then plotted versus the frequency of $CD8^+$ IFN-γ^+ T cells for each epitope (Fig. 8B). The curve represents the fit of a rate equation model, assuming a rate of specific killing proportional to the number of antigen-specific $CD8^+$ IFN-γ^+ T cells times the number of peptide-pulsed target cells. Overall, a positive correlation was observed between the level of cytotoxicity and IFN-γ production for the majority of epitopes. However, three outlying epitopes, L349-357, L455-463, and NP165-175, on the lower right of Fig. 8B were not included in the model fit. Interestingly, these outlying T-cell subsets produced significant levels of IFN-γ but only generated low levels of in vivo killing.

Protection from LCMV challenge is dependent on the level of in vivo cytotoxicity. Since epitopes derived from the L protein were effective at generating IFN-γ and TNF-α responses as well as inducing significant levels of cytotoxicity, we examined whether priming of B6 mice with L peptides would confer protection against a subsequent virus challenge. B6 mice were immunized with GP33-41, L2062-2069, L156-163, L455-463, or a mock control with DMSO. Twelve days after peptide immunization, mice were challenged i.p. with a 1×10^5-PFU dose of LCMV Armstrong. As shown in Fig. 8C, priming the mice with GP33-41 peptide conferred protection against LCMV challenge. Protection against infection was also seen for the L epitope, L2062-2069. For both GP33-41 and L2062-2069 peptide-primed mice, significant reductions in virus titers at day 4 postinfection were observed (Fig. 8C). L156-163 peptide-primed mice were only moderately protected following virus challenge. In contrast, the L455-463 peptide-primed and mock-primed mice were not able to control LCMV infection.

We then determined whether the protective capacity of the L peptides was dependent on the cytolytic activity and/or IFN-γ production of the L-specific CTLs. For L2062-2069, L156-163, and L455-463 epitopes, we observed that viral load in peptide-primed mice was inversely correlated with the cytolytic activity of the L-specific $CD8^+$ T cells. Furthermore, the protective capacity of the L peptides seemed independent of IFN-γ production since L2062-2069- and L455-463-specific $CD8^+$ T cells produced moderate and high amounts of IFN-γ, respectively, but vastly differed in their protective capacity. Thus, priming with a peptide derived from the L protein can confer protective immunity to virus challenge and is largely dependent on the cytotoxic potential of the L-specific $CD8^+$ T cells.

DISCUSSION

In this study, we performed a comprehensive screen of the entire LCMV Armstrong proteome, including the GP, NP, L, and Z proteins, with the main purpose of reexamining immunodominance in the LCMV system. This reevaluation was prompted by the observation that a significant fraction of the $CD44^{hi}$-specific $CD8^+$ T-cell response was not accounted for by known epitopes. These comprehensive analyses confirmed the antigenicity of previously characterized epitopes from GP and NP, and at the same time, identified four new epitopes from the GP protein. Two of the 11-mer NP epitopes, NP165-175 and NP238-248, overlapped with the two NP 15-mer peptides documented in a recent study by van der Most et al., where the antigenicity of 15-mer peptides spanning LCMV Armstrong GP and NP was examined by IFN-γ ICCS (31). No epitope was identified from the Z protein, probably because of its small size (~99 amino acids). Strikingly, a total of 15 novel epitopes from the RNA polymerase L protein, not previously believed to be antigenic, were identified here. The identification of these new epitopes, the majority of which were derived from the L protein, demonstrates that the overall breadth of the LCMV-specific $CD8^+$ T-cell response is more complex than previously appreciated.

The identification of novel LCMV-derived epitopes raised the question of functional significance of each of these epitopes during LCMV infection of $H\text{-}2^b$ mice. We addressed this by comparing the characteristics of the known epitopes to the newly defined epitopes through several different functional assays. We found that the new epitopes induced responses of similar magnitude and have TCR peptide avidities, primary TNF-α responses, and memory IFN-γ responses similar to those of the previously characterized epitopes. Several of the new epitopes, including four L epitopes, induced significant levels of in vivo cytotoxicity. We found that there was an overall positive correlation between IFN-γ production and cytolytic activity. However, not all epitopes fit this model, suggesting that in some cases IFN-γ production is independent of CTL activity. This phenomenon might be linked to peptide avidity for either MHC or T-cell receptor (TCR) molecules. By extending this comparison to the protective capacity of the L peptides, we observed that L peptides could confer protection if the corresponding L-specific CTLs had high cytolytic potential. Interestingly, the protective capacity of the L peptides appeared to be largely independent of IFN-γ production. In addition, it appears that in some instances cytotoxicity and protection might not always be correlated with TCR peptide avidity. For example, the L2062 peptide appears to have a high affinity to the K^b molecule (1.1 nM) but a low avidity to the TCR. Even with the low TCR avidity, the L2062 peptide triggered the strongest killing and the highest level of protection of the three L peptides tested. Taken together, this suggests that the L peptides are present in sufficient quantities during LCMV infection and reinforces the functional importance of the L-specific $CD8^+$ T-cell response.

In this study, we also observed unrealistically large $CD8^+$ T-cell responses directed against LCMV when using high doses of stimulating peptide. For instance, adding together individual $CD8^+$ T-cell responses produced with 1 μg/ml of peptide in IFN-γ ICCS assays led to nonrealistic estimates of total responses that were greater than 110% of $CD8^+$ T cells. Thus, when measuring $CD8^+$ T-cell frequencies, high peptide concentrations should be interpreted with care (6, 15) and lower doses might be more physiologically relevant (2). Accordingly, in our study, when characterizing the novel epitopes, we ensured that high peptide concentrations were not used.

When determining the total LCMV-specific $CD8^+$ T-cell response, we found that the percentage of activated $CD8^+$ $CD44^{hi}$ T cells generated against LCMV was in the 87 to 95% range. This is in agreement with a recent study that used $CD44^{hi}$ expression along with granzyme B, 1B11, CD62L, CD11a, and CD127 expression to estimate the number of ac-

tivated $CD8^+$ T cells in LCMV-infected B6 mice, where approximately 85 to 95% of $CD8^+$ T cells exhibited an effector phenotype at day 8 postinfection (17). Total virus-specific $CD8^+$ T-cell responses have also been estimated by using virus-infected MHC class I-matched cells as stimulators (13, 19). Nevertheless, in the case of LCMV infection of H-2^b mice, no information is available, and as we found, the results with infected cells were highly variable (data not shown). Alternatively, the total LCMV-specific response has been estimated by adding individual epitope-specific $CD8^+$ T-cell responses (20). Overall, we found that the percentage of $CD8^+$ $CD44^{hi}$ T cells closely correlated with the epitope-specific response when using individual peptides at low doses, thus suggesting that there is very little bystander T-cell activation during acute LCMV infection and that the greater part of the $CD8^+$ T-cell response to LCMV was mapped in this study.

Prior to this study, H-2^b-restricted epitopes derived from the L protein had not been reported. One previous study intimated that H-2^b mice infected with a viral variant of LCMV Armstrong mounted $CD8^+$ T-cell responses against the L protein; however, no L-specific epitopes were documented (16). Therefore, we were surprised by the large number of L epitopes identified in our study. In fact, a significant portion of the overall LCMV-specific $CD8^+$ T-cell response was "hidden" within the L protein. Supporting our findings, a recent study has identified an H-2^d-restricted epitope located within the L protein, further demonstrating L protein antigenicity (5). The antigenicity of the L protein has been generally discounted because of early reports on the low level of mRNA transcription and protein expression of the polymerase both in vitro and in vivo (10–12). Furthermore, L epitopes have been overlooked in previous studies searching for novel LCMV-derived epitopes, since these studies only focused on the antigenicity of GP and NP and did not extend their analysis over the entire LCMV proteome (31, 32). The unearthing of L epitopes suggests that proteins made in small quantities during viral infection are capable of being recognized and inducing a substantial $CD8^+$ T cell response.

Our study also allows a side-by-side comparison of two popular epitope identification methods, namely, MHC binding prediction and overlapping 15-mer peptides. Only the top 160 peptides were required to capture all of the antigenic peptides found by the predictive method. Fewer peptides were required in comparison to the overlapping peptide approach, but the predictive approach was unable to identify epitopes greater than 10 amino acids in length or determinants containing noncanonical K^b or D^b binding motifs. The overlapping peptide approach identified a smaller fraction of the overall response (approximately 65% compared to 89%). In addition, a larger number of peptides were initially screened, and several hundreds of peptides were required to map the minimal epitope within each positive 15-mer.

We established that the overall breadth of $CD8^+$ T-cell responses against LCMV is broader than previously thought. Based on these results, current models for T-cell specificity and immunodominance should be adjusted to include the newly defined epitopes. Taken together, the data presented in this study illustrates that even though LCMV infection of H-2^b mice is one of the most well-characterized systems for studying viral infection, new aspects of the virus interaction with its host continue to be discovered.

ACKNOWLEDGMENTS

We are grateful to T. J. Pencille, Fred Montoya, and Carrie Moore for the MHC binding assays and Edith Janssen, Sonia Feau, Marta Lopez Fraga, Diane Rottembourg, Polly Barrowman, and Tom Wolfe for their technical assistance. We also thank Bianca Mothe and Valerie Pasquetto for valuable discussions and comments on the manuscript.

This study was supported by the National Institutes of Health grants AI065359 (to J.B. and M.J.B.) and contract NO1-AI-40023 (to A.S.).

REFERENCES

1. **Addo, M. M., X. G. Yu, A. Rathod, D. Cohen, R. L. Eldridge, D. Strick, M. N. Johnston, C. Corcoran, A. G. Wurcel, C. A. Fitzpatrick, M. E. Feeney, W. R. Rodriguez, N. Basgoz, R. Draenert, D. R. Stone, C. Brander, P. J. Goulder, E. S. Rosenberg, M. Altfeld, and B. D. Walker.** 2003. Comprehensive epitope analysis of human immunodeficiency virus type 1 (HIV-1)-specific T-cell responses directed against the entire expressed HIV-1 genome demonstrate broadly directed responses, but no correlation to viral load. J. Virol. **77:**2081–2092.
2. **Badovinac, V. P., and J. T. Harty.** 2000. Intracellular staining for TNF and IFN-gamma detects different frequencies of antigen-specific CD8(+) T cells. J. Immunol. Methods **238:**107–117.
3. **Basler, M., N. Youhnovski, M. Van Den Broek, M. Przybylski, and M. Groettrup.** 2004. Immunoproteasomes down-regulate presentation of a subdominant T cell epitope from lymphocytic choriomeningitis virus. J. Immunol. **173:**3925–3934.
4. **Bharadwaj, M., M. Sherritt, R. Khanna, and D. J. Moss.** 2001. Contrasting Epstein-Barr virus-specific cytotoxic T cell responses to HLA A2-restricted epitopes in humans and HLA transgenic mice: implications for vaccine design. Vaccine **19:**3769–3777.
5. **Botten, J., J. L. Whitton, P. Barrowman, J. Sidney, J. K. Whitmire, J. Alexander, J. P. Ting, H. H. Bui, A. Sette, and M. J. Buchmeier.** 2007. HLA-A2-restricted protection against lethal lymphocytic choriomeningitis. J. Virol. **81:**2307–2317.
6. **Brehm, M. A., T. G. Markees, K. A. Daniels, D. L. Greiner, A. A. Rossini, and R. M. Welsh.** 2003. Direct visualization of cross-reactive effector and memory allo-specific CD8 T cells generated in response to viral infections. J. Immunol. **170:**4077–4086.
7. **Butz, E. A., and M. J. Bevan.** 1998. Massive expansion of antigen-specific CD8+ T cells during an acute virus infection. Immunity **8:**167–175.
8. **Doolan, D. L., S. Southwood, D. A. Freilich, J. Sidney, N. L. Graber, L. Shatney, L. Bebris, L. Florens, C. Dobano, A. A. Witney, E. Appella, S. L. Hoffman, J. R. Yates III, D. J. Carucci, and A. Sette.** 2003. Identification of Plasmodium falciparum antigens by antigenic analysis of genomic and proteomic data. Proc. Natl. Acad. Sci. USA **100:**9952–9957.
9. **Elkington, R., S. Walker, T. Crough, M. Menzies, J. Tellam, M. Bharadwaj, and R. Khanna.** 2003. Ex vivo profiling of CD8+-T-cell responses to human cytomegalovirus reveals broad and multispecific reactivities in healthy virus carriers. J. Virol. **77:**5226–5240.
10. **Francis, S. J., M. K. Singh, M. B. Oldstone, and P. J. Southern.** 1986. Analysis of lymphocytic choriomeningitis virus gene expression in acutely and persistently infected mice. Med. Microbiol. Immunol. (Berlin) **175:**105–108.
11. **Francis, S. J., P. J. Southern, A. Valsamakis, and M. B. Oldstone.** 1987. State of viral genome and proteins during persistent lymphocytic choriomeningitis virus infection. Curr. Top. Microbiol. Immunol. **133:**67–88.
12. **Fuller-Pace, F. V., and P. J. Southern.** 1989. Detection of virus-specific RNA-dependent RNA polymerase activity in extracts from cells infected with lymphocytic choriomeningitis virus: in vitro synthesis of full-length viral RNA species. J. Virol. **63:**1938–1944.
13. **Harrington, L. E., R. van der Most, J. L. Whitton, and R. Ahmed.** 2002. Recombinant vaccinia virus-induced T-cell immunity: quantitation of the response to the virus vector and the foreign epitope. J. Virol. **76:**3329–3337.
14. **Jameson, J., J. Cruz, and F. A. Ennis.** 1998. Human cytotoxic T-lymphocyte repertoire to influenza A viruses. J. Virol. **72:**8682–8689.
15. **Kim, S. K., M. Cornberg, X. Z. Wang, H. D. Chen, L. K. Selin, and R. M. Welsh.** 2005. Private specificities of CD8 T cell responses control patterns of heterologous immunity. J. Exp. Med. **201:**523–533.
16. **Lewicki, H. A., M. G. Von Herrath, C. F. Evans, J. L. Whitton, and M. B. Oldstone.** 1995. CTL escape viral variants. II. Biologic activity in vivo. Virology **211:**443–450.
17. **Masopust, D., K. Murali-Krishna, and R. Ahmed.** 2007. Quantitating the magnitude of the lymphocytic choriomeningitis virus-specific CD8 T-cell response: it is even bigger than we thought. J. Virol. **81:**2002–2011.
18. **Milich, D. R., J. L. Hughes, A. McLachlan, G. B. Thornton, and A. Moriarty.** 1988. Hepatitis B synthetic immunogen comprised of nucleocapsid T-cell sites and an envelope B-cell epitope. Proc. Natl. Acad. Sci. USA **85:**1610–1614.

19. **Moutaftsi, M., B. Peters, V. Pasquetto, D. C. Tscharke, J. Sidney, H. H. Bui, H. Grey, and A. Sette.** 2006. A consensus epitope prediction approach identifies the breadth of murine T(CD8+)-cell responses to vaccinia virus. Nat. Biotechnol. **24:**817–819.
20. **Murali-Krishna, K., J. D. Altman, M. Suresh, D. J. Sourdive, A. J. Zajac, J. D. Miller, J. Slansky, and R. Ahmed.** 1998. Counting antigen-specific CD8 T cells: a reevaluation of bystander activation during viral infection. Immunity **8:**177–187.
21. **Oseroff, C., F. Kos, H. H. Bui, B. Peters, V. Pasquetto, J. Glenn, T. Palmore, J. Sidney, D. C. Tscharke, J. R. Bennink, S. Southwood, H. M. Grey, J. W. Yewdell, and A. Sette.** 2005. HLA class I-restricted responses to vaccinia recognize a broad array of proteins mainly involved in virulence and viral gene regulation. Proc. Natl. Acad. Sci. USA **102:**13980–13985.
22. **Pasquetto, V., H. H. Bui, R. Giannino, C. Banh, F. Mirza, J. Sidney, C. Oseroff, D. C. Tscharke, K. Irvine, J. R. Bennink, B. Peters, S. Southwood, V. Cerundolo, H. Grey, J. W. Yewdell, and A. Sette.** 2005. HLA-A*0201, HLA-A*1101, and HLA-B*0702 transgenic mice recognize numerous poxvirus determinants from a wide variety of viral gene products. J. Immunol. **175:**5504–5515.
23. **Peters, B., and A. Sette.** 2005. Generating quantitative models describing the sequence specificity of biological processes with the stabilized matrix method. BMC Bioinformatics **6:**132.
24. **Probst, H. C., K. Tschannen, A. Gallimore, M. Martinic, M. Basler, T. Dumrese, E. Jones, and M. F. van den Broek.** 2003. Immunodominance of an antiviral cytotoxic T cell response is shaped by the kinetics of viral protein expression. J. Immunol. **171:**5415–5422.
25. **Sette, A., A. Vitiello, B. Reherman, P. Fowler, R. Nayersina, W. M. Kast, C. J. Melief, C. Oseroff, L. Yuan, J. Ruppert, et al.** 1994. The relationship between class I binding affinity and immunogenicity of potential cytotoxic T cell epitopes. J. Immunol. **153:**5586–5592.
26. **Sidney, J., S. Southwood, C. Oseroff, M. F. D. Guercio, A. Sette, and H. Grey.** 1998. Measurement of MHC/peptide interactions by gel filtration, p. 18.3.1–18.3.19. *In* J. E. Coligan, A. M. Kruisbeek, D. H. Margulies, E. M. Shevach, and W. Strober (ed.), Current protocols in immunology, vol. I. John Wiley & Sons, New York, NY.
27. **Sylwester, A. W., B. L. Mitchell, J. B. Edgar, C. Taormina, C. Pelte, F. Ruchti, P. R. Sleath, K. H. Grabstein, N. A. Hosken, F. Kern, J. A. Nelson, and L. J. Picker.** 2005. Broadly targeted human cytomegalovirus-specific CD4+ and CD8+ T cells dominate the memory compartments of exposed subjects. J. Exp. Med. **202:**673–685.
28. **Tangri, S., G. Y. Ishioka, X. Huang, J. Sidney, S. Southwood, J. Fikes, and A. Sette.** 2001. Structural features of peptide analogs of human histocompatibility leukocyte antigen class I epitopes that are more potent and immunogenic than wild-type peptide. J. Exp. Med. **194:**833–846.
29. **Tewari, K., J. Sacha, X. Gao, and M. Suresh.** 2004. Effect of chronic viral infection on epitope selection, cytokine production, and surface phenotype of CD8 T cells and the role of IFN-gamma receptor in immune regulation. J. Immunol. **172:**1491–1500.
30. **Udaka, K., K. H. Wiesmuller, S. Kienle, G. Jung, H. Tamamura, H. Yamagishi, K. Okumura, P. Walden, T. Suto, and T. Kawasaki.** 2000. An automated prediction of MHC class I-binding peptides based on positional scanning with peptide libraries. Immunogenetics **51:**816–828.
31. **van der Most, R. G., K. Murali-Krishna, J. G. Lanier, E. J. Wherry, M. T. Puglielli, J. N. Blattman, A. Sette, and R. Ahmed.** 2003. Changing immunodominance patterns in antiviral CD8 T-cell responses after loss of epitope presentation or chronic antigenic stimulation. Virology **315:**93–102.
32. **van der Most, R. G., K. Murali-Krishna, J. L. Whitton, C. Oseroff, J. Alexander, S. Southwood, J. Sidney, R. W. Chesnut, A. Sette, and R. Ahmed.** 1998. Identification of Db- and Kb-restricted subdominant cytotoxic T-cell responses in lymphocytic choriomeningitis virus-infected mice. Virology **240:**158–167.
33. **Yewdell, J. W., and J. R. Bennink.** 1999. Immunodominance in major histocompatibility complex class I-restricted T lymphocyte responses. Annu. Rev. Immunol. **17:**51–88.